DNA break formation induces Scc2/cohesin-dependent recruitment of condensin to meiotic chromosomes

Tovah E. Markowitz[1,#], Jonna Heldrich[1], and Andreas Hochwagen[1,*]

[1] Department of Biology, New York University; New York, NY; USA

[#] Current address: Leidos Biomedical Research, Inc.; Bethesda, MD; USA

[*] Correspondence: andi@nyu.edu

Running title: Condensin recruitment during meiotic prophase

Key words: Axial element, synapsis, Smc4, Spo11, Rec8

Abstract

Meiotic chromosome pairing, recombination, and fertility depends on the conserved loop-axis architecture of meiotic chromosomes. This architecture is modulated by condensin, a structural maintenance of chromosome (SMC) complex that catalyzes chromatin loop formation. Here, we investigated how condensin is recruited to meiotic chromosomes in *Saccharomyces cerevisiae*. We show that double-strand-break (DSB) formation, the initiating event of meiotic recombination, causes condensin redistribution from the nucleolus to DSB hotspots, pericentromeric regions, and axis attachment sites. Hotspot association of condensin correlates weakly with break probability but does not depend on local DSB formation, whereas association with axis sites and pericentromeric regions depends on the Scc2-associated pool of cohesin, another SMC complex. Intriguingly, Scc2 distribution also changes in response to DSB formation. As condensin and Scc2-cohesin both catalyze chromatin loop extrusion, their redistribution upon DSB formation implies a profound change in chromatin loop dynamics that may help promote proper chromosome pairing and DNA repair.

Introduction

Higher-order chromosome architecture allows cells to organize and maneuver large sections of chromatin to modulate gene expression, support DNA metabolism, and enable chromosome segregation (Bickmore and van Steensel, 2013, Hildebrand and Dekker, 2020). The structural compartmentalization of chromosomes also plays a key role during meiotic recombination (Zickler and Kleckner, 2015). During meiotic prophase, chromosomes reorganize into linear arrays of chromatin loops along a nucleoprotein axis, known as the axial element. This loop-axis arrangement is of central importance for controlling meiotic recombination. It promotes recombination initiation by stimulating the formation of meiotic DNA double-strand breaks (DSBs), helps properly target DSBs for homologous repair, and provides a platform for damage surveillance and checkpoint control (Zickler and Kleckner, 2015, Subramanian et al., 2019). Mutations that disrupt the axial element lead to severe defects in meiotic recombination and chromosome segregation and cause male infertility and premature ovarian failure in humans (Llano et al., 2014, Caburet et al., 2014, Geisinger and Benavente, 2016).

The chromosomal translocases condensin and cohesin are central regulators of higher-order chromosome organization in mitosis and meiosis (Yatskevich et al., 2019, Uhlmann, 2016). Both complexes belong to the Structural Maintenance of Chromosomes (SMC) family of protein complexes, which can encircle chromatin through a ring-shaped binding interface, formed by two SMC ATPases and a kleisin linker protein. With the help of additional subunits, both complexes have the ability to promote the ATP-dependent formation of DNA loops, most probably by extruding chromatin through their rings (Hassler et al., 2018, van Ruiten and Rowland, 2018). Condensin and cohesin differ in their relative residence time on chromatin. Whereas condensin association patterns are consistent with repeated on-and-off cycles (Thadani et al., 2018), cohesin also has the capacity to remain stably associated with chromatin for extended periods of time, likely by associating with different regulatory subunits (Yatskevich et al., 2019, Petela et al., 2018).

Cohesin and condensin have important roles in organizing the architecture of meiotic chromosomes. Cohesin is an essential building block of the axial element (Klein et al., 1999) and topologically links the axial element to chromatin (Sun et al., 2015, Glynn et al., 2004). Loss of cohesin function in meiotic prophase has been studied extensively and affects numerous aspects of meiotic recombination, chromosome pairing, and nuclear architecture (Klein et al., 1999, Brar et al., 2009, Kim et al., 2010, Jin et al., 2009, Kugou et al., 2009, Trelles-Sticken et al., 2005, McNicoll et al., 2013). The roles of condensin during meiotic prophase remain less defined. Like cohesin, condensin is found enriched at

axial cores of meiotic chromosomes by cytology (Viera et al., 2007, Yu and Koshland, 2003) and plays an important role in the formation of the synaptonemal complex (SC), a ladder-like nucleoprotein assembly that connects homologous chromosome pairs in the process of recombination (Hernandez et al., 2018, Yu and Koshland, 2003). In addition, condensin regulates DSB formation in *C. elegans* (Hernandez et al., 2018, Mets and Meyer, 2009) and suppresses illicit recombination of repetitive DNA in *S. cerevisiae* and *S. pombe* (Li et al., 2014, Johansen and Cam, 2015).

Both, cohesin and condensin depend on recruitment factors for chromosomal association. Cohesin binding along chromosomes requires the loading factor Scc2/NIPBL (Ciosk et al., 2000), which stably binds to cohesin and also hops between chromatin-associated cohesin complexes to stimulate their ATPase activity (Petela et al., 2018, Rhodes et al., 2017). By contrast, condensin likely relies on several different recruitment mechanisms. For example, condensin enrichment at tRNA genes requires the transcription factor TFIIIC (D'Ambrosio et al., 2008), enrichment at centromeres and the ribosomal DNA (rDNA) involves the monopolin complex (Johzuka and Horiuchi, 2009, Tada et al., 2011, Burrack et al., 2013), and binding to mitotic chromosomes requires phosphorylation of histones H2A and H2A.Z (Tada et al., 2011). Scc2 has also been implicated as a loader of condensin in *S. cerevisiae* (D'Ambrosio et al., 2008), although this association has remained controversial (Shen and Skibbens, 2017) and has not been found in other organisms (Lightfoot et al., 2011). The mechanisms that recruit condensin to chromosomes during meiotic prophase have remained largely unclear.

Here, we analyzed meiotic condensin recruitment in *S. cerevisiae*. Consistent with previous analyses (Yu and Koshland, 2003), we found that condensin relocalizes from the nucleolus to meiotic chromosome axes in the course of meiotic prophase. Release from the nucleolus requires the induction of meiotic DSBs, whereas association with axis attachment sites depends on the meiotic cohesin subunit Rec8 and the activating cohesin subunit Scc2. The enrichment of both, condensin and Scc2, shifts from pericentromeric regions to axis attachment sites in response to DSBs, revealing the combined redeployment of two regulators of loop extrusion in response to meiotic DSB formation.

Results

Dynamic redistribution of condensin during meiotic prophase

To investigate the dynamics of condensin in meiotic prophase, we induced cells to undergo a synchronous meiotic time course and analyzed the distribution of the condensin SMC subunit Smc4

fused to GFP on spread prophase chromosomes. At early time points (2h; corresponding to premeiotic S phase under our conditions (Blitzblau et al., 2012)), Smc4-GFP was primarily enriched on the rDNA as indicated by a cluster of foci near the nucleolar marker Nop1. Some cells also showed foci on non-nucleolar chromatin (**Figure 1A-B**). As cells progressed into meiotic prophase and initiated formation of the SC, the nucleolar enrichment progressively weakened and condensin formed foci that localized on or near the SC protein Zip1. By late prophase (4h), the distinct nucleolar enrichment was no longer detectable, and Smc4-GFP formed numerous foci along the mature SC (**Figure 1B** and **S1A**). We failed to see the extensive axial staining observed in a previous study (Yu and Koshland, 2003), but note that those analyses were performed after long prophase arrest, which may lead to a buildup of condensin along the SC.

The dynamics of condensin distribution suggested that condensin binding is coordinated with meiotic recombination. To test this possibility, we analyzed catalytically inactive *spo11-Y135F* (*spo11-YF*) mutants, which are unable to initiate meiotic DSB formation (Bergerat et al., 1997, Keeney et al., 1997). In these mutants, Smc4-GFP did not exhibit the progressive association with chromosomes seen in wild type (**Figure 1B** and **S1B**), indicating that condensin redistribution depends on the initiation of meiotic recombination.

The colocalization of condensin foci with the SC also implied a role for meiotic chromosome architecture in condensin recruitment. Previous cytological analyses showed that condensin recruitment to meiotic chromosome axes occurs independently of Zip1 and the axial-element proteins Red1 and Hop1 (Yu and Koshland, 2003). As chromosomal recruitment of all three proteins requires the cohesin Rec8 (Klein et al., 1999), we analyzed Smc4-GFP in *rec8*Δ mutants. Similar to wild type, chromosome spreads of *rec8*Δ mutants showed a progressive loss of nucleolar condensin as cells progressed into meiotic prophase (**Figure 1A-B** and **S1C**). However, some nucleolar clusters remained even at 4h, possibly because the lower levels of DSB formation in these mutants (Kugou et al., 2009, Markowitz et al., 2017) lead to less efficient condensin dissociation from the nucleolus. Importantly, the loss of nucleolar enrichment was not accompanied by accumulation of condensin on chromosomes, resulting in a growing fraction of cells without GFP signal. At earlier time points, total signal intensity of chromosome spreads with detectable Smc4-GFP signal was not significantly different between wild type, *spo11-YF* mutants and *rec8*Δ mutants (**Figure 1C**), indicating that the changes in condensin patterns are primarily the result of condensin redistribution, rather than differential condensin expression. We conclude that meiotic DSB formation causes a loss of nucleolar enrichment of

condensin, and that Rec8-dependent chromosome architecture provides binding sites for condensin upon DSB formation.

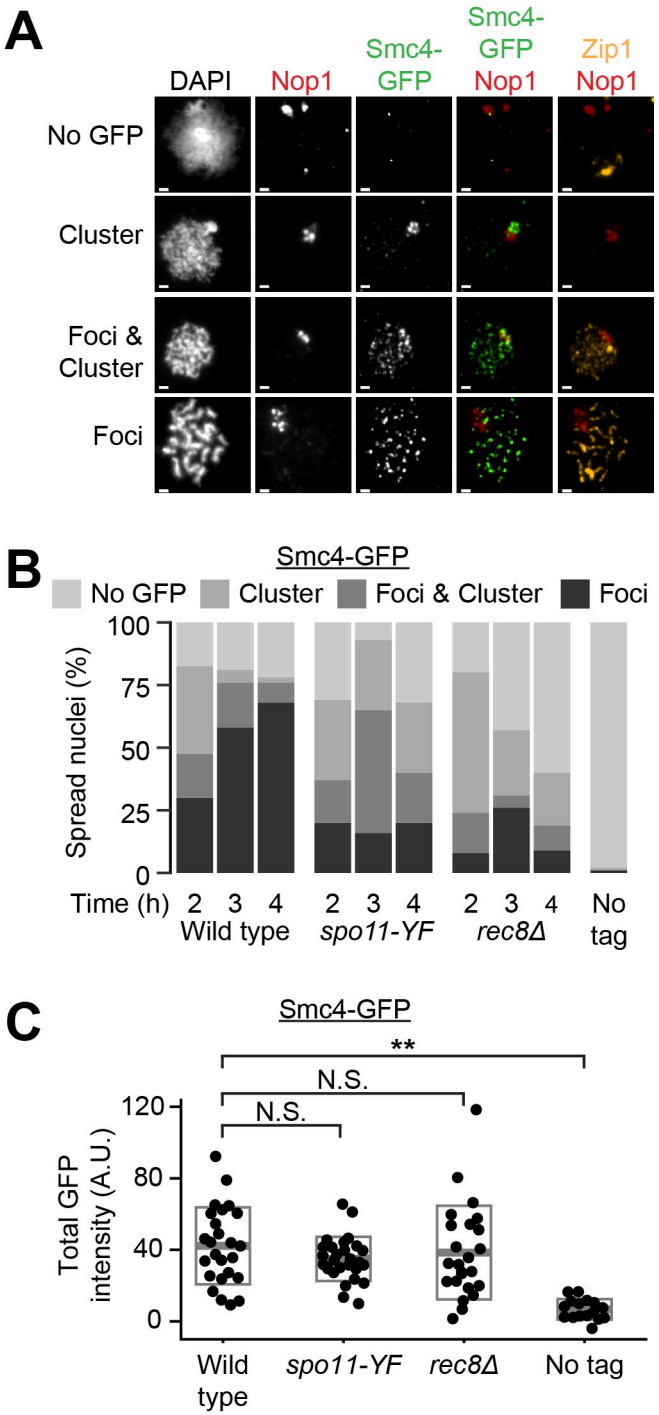

Figure 1. Condensin distribution on prophase chromosomes depends on *SPO11* and *REC8*. (A) Representative images of Nop1 (red), Smc4-GFP (green), and Zip1 (orange) binding patterns on surface-spread nuclei, showing "No GFP", "Foci", "Foci & Cluster", or "Cluster" patterns of GFP. **(B)** Counts of GFP patterns on chromosome spreads in wild-type [H9443], *rec8*Δ [H9442], *spo11-YF* [H9441], or in the absence of a GFP tag ("no tag") [H7797], n=100. **(C)** Quantifications of GFP levels

on wild-type, *rec8*Δ, *spo11-YF*, or untagged control nuclei 3h after meiotic induction. Only nuclei with visible Zip1 staining were analyzed, n=25, 24, 27, 16 respectively. Total GFP intensity for each nucleus was normalized against a background region of equal size. Bars indicate mean and S.D. **: p-value < 10^{-5}, N.S.: not significant; Wilcox test.

Condensin is enriched in pericentromeric regions in meiotic prophase

To determine the chromosomal distribution of condensin with higher spatial resolution, we analyzed epitope-tagged Smc4 (Smc4-PK9 (D'Ambrosio et al., 2008)) by chromatin immunoprecipitation and sequencing (ChIP-seq). Synchronous cell populations were collected 3h after meiotic induction, corresponding to mid-prophase under our experimental conditions (Falk et al., 2010).

Initial experiments using a standard ChIP-seq protocol failed to recover specific peaks of condensin enrichment when compared to a no-tag control (**Figure S2A**). The only exception was a specific peak in the rDNA (**Figure S2B**). This recovery problem appeared to be linked to poor fragmentation of condensin-associated chromatin. Our library preparation protocol excludes DNA fragments >500bp, because large fragments are less efficiently amplified on the Illumina platform. Protein binding, however, can alter DNA fragmentation patterns during sonication (Auerbach et al., 2009), which could result in large DNA fragments that would not be sequenced. To test this possibility, we proteolytically eliminated all proteins after the immunoprecipitation step and re-sonicated the pure DNA fragments prior to library preparation. Similar approaches have been used to detect broad histone marks over background in human cell lines (Laczik et al., 2016). This approach led to the recovery of numerous specific peaks of Smc4-PK9 enrichment. These peaks were not observed in a similarly treated control strain lacking the PK9 tag, indicating these signals are specific to condensin (**Figure S2C**). Consistent with this interpretation, binding profiles of Smc4-PK9 from re-sonicated meiotic samples exhibited several features also seen in vegetative cells, including enrichment at tRNA genes, the ribosomal DNA (rDNA) (Wang et al., 2005, D'Ambrosio et al., 2008), and in the immediate vicinity (<2kb) of centromeres (Wang et al., 2005) (**Figures 2A-B** and **S2D-E**).

Intriguingly, meiotic prophase chromosomes also exhibited patterns of condensin enrichment that, in vegetative cells, are only observed during mitosis (D'Ambrosio et al., 2008, Verzijlbergen et al., 2014). These include substantial peaks of condensin enrichment in the pericentromeric regions (within 10kb of a centromere) (**Figure 2A-B**) and regional enrichment of condensin between *CEN12* and the rDNA (**Figure S2F**). The latter enrichment pattern is prominently observed as a domain of enrichment to the

right of *CEN12* in vegetative cells (arrow, **Figure 2A**) and is linked to the establishment of a topologically associated domain that is thought to only form in anaphase (Paul et al., 2018, Lazar-Stefanita et al., 2017, Schalbetter et al., 2017). These mitotic-like patterns of condensin association may reflect the high degree of chromosomal compaction seen during meiotic prophase (Yu and Koshland, 2003).

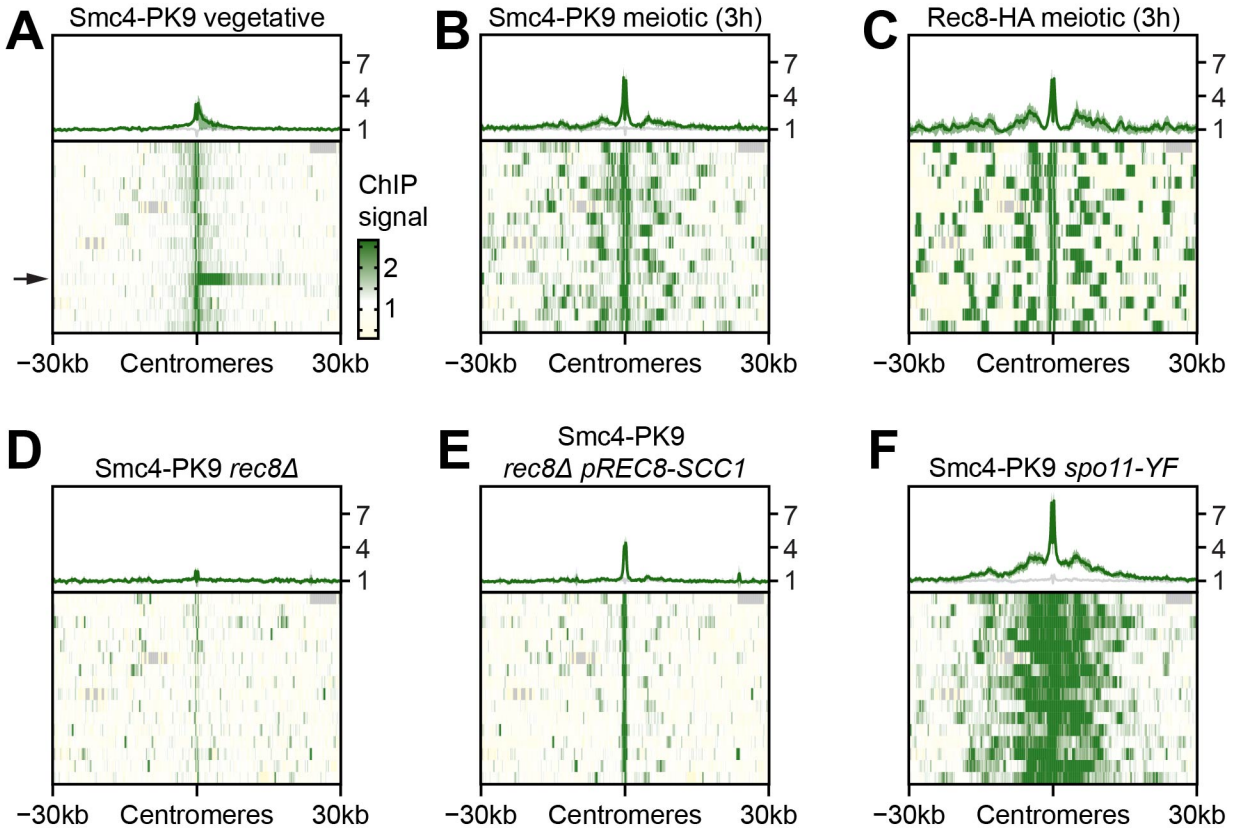

Figure 2. Condensin binding pattern at pericentromeres depends on *REC8* and *SPO11*. Heatmaps around pericentromeres of: Smc4-PK9 enrichment from vegetative cells [H6408] **(A)**, Smc4-PK9 enrichment in meiotic prophase [H6408] (t=3h) **(B)**, Rec8-HA enrichment in meiotic prophase (t=3h) [H4471] **(C)**, Smc4-PK9 enrichment in a *rec8*Δ mutant [H7660] (t=3h) **(D)**, Smc4-PK9 enrichment in a *rec8*Δ *pREC8-SCC1* [H8921] (t=3h) **(E)**, and Smc4-PK9 enrichment in a *spo11-YF* mutant [H8630] (t=3h) **(F)**. Arrow in (A) indicates the pericentromeric regions flanking *CEN12*. ChIP-seq fold enrichment values were averaged over 100bp windows across a 60kb window centered on centromere midpoints. Rows are sorted by chromosome number. Green indicates high enrichment. Mean and S.E.M. are shown in line graph directly above heatmap. Gray lines indicate mean and S.E.M. of the no-tag controls: H7797 (A), H7797 (B), H8428 (D), H8038 (E), and H8643 (F).

Condensin binding to pericentromeric regions requires cohesin

The enrichment pattern of Smc4-PK9 in pericentromeric regions during meiotic prophase was similar to the distribution of the meiosis-specific cohesin subunit Rec8, the kleisin that replaces the mitotic kleisin Scc1 in meiotic cohesin complexes (**Figure 2B-C**). To test whether cohesin is responsible for condensin recruitment, we performed Smc4-PK9 ChIP-seq analysis in *rec8*Δ mutants. Pericentromeric condensin enrichment was completely abolished in *rec8*Δ mutants, although some enrichment remained detectable near the core centromeres (**Figure 2D**). These data are consistent with the dependence on *REC8* observed by cytology (**Figure 1B** and **S1C**). The binding of condensin at tRNA genes was unaffected in *rec8* mutants (**Figure S3A**), consistent with a separate recruitment mechanism (D'Ambrosio et al., 2008).

To test whether recruitment depends on Rec8 itself or the formation of the cohesin ring, we analyzed Smc4-PK9 binding in a *pREC8-SCC1 rec8*Δ mutant. In these cells, the mitotic kleisin Scc1 is expressed instead of Rec8 during meiosis, allowing cohesin to bind to its traditional binding sites along the genome (Sun et al., 2015). Expression of Scc1 partially restored condensin enrichment at core centromeres and led to weak but detectable condensin enrichment in the pericentromeric regions that resembled the pattern of wild-type cells (**Figure 2E**). These data indicate that although ectopic Scc1 expression cannot fully substitute for Rec8, mitotic Scc1-cohesin is able to recruit some condensin to meiotic pericentromeres.

Pericentromeric condensin redistributes in response to DSB formation

As our cytological analyses had indicated a role for DSB formation in condensin redistribution to chromosomes (**Figure 1B** and **S1B**), we also performed ChIP-seq analysis of Smc4-PK9 in *spo11-YF* mutants. In the absence of DSBs, binding at tRNA genes was largely abolished (**Figure S3B**) and the defined enrichment pattern of Smc4-PK9 in the pericentromeric regions was replaced by a strong enrichment signal around the core centromere (**Figure 2F**). The same strong enrichment around centromeres was also observed in *spo11*Δ mutants (**Figure S3C**). These data indicate that DSB formation influences the relative distribution of condensin in pericentromeric regions.

Cohesin-dependent enrichment of condensin at axis attachment sites

We also observed meiosis-specific condensin enrichment at meiotic axis attachment sites. Axis attachment sites represent chromatin interfaces with the axial element and are defined by strong local enrichment of Rec8 and the axial-element factor Red1 (Sun et al., 2015, Glynn et al., 2004, Schalbetter

et al., 2019). They are most frequently found near the ends of convergently transcribed genes and largely coincide with cohesin-attachment regions defined in vegetative cells (Sun et al., 2015, Glynn et al., 2004, Lengronne et al., 2004, Ocampo-Hafalla et al., 2016). Although Smc4-PK9 peaks visibly outnumbered the peaks of Rec8 and Red1, almost all axis Rec8 and Red1 peaks overlapped with Smc4-PK9 peaks (**Figure 3A** and **S4A)**. Accordingly, Smc4-PK9 was strongly enriched at axis sites (**Figure 3B**) and tracked the distribution of Red1 near convergent gene ends (**Figure S4B-C**), indicating that condensin binds to axis attachment sites during meiotic prophase.

To test whether condensin enrichment at axis sites requires cohesin, we analyzed Smc4-PK9 binding in *rec8*Δ and *pREC8-SCC1 rec8*Δ strains. This analysis recapitulated the genetic dependencies seen at pericentromeres; condensin enrichment at axis sites was abolished in *rec8*Δ mutants and was partially restored in *pREC8-SCC1 rec8*Δ mutants (**Figure 3B** and **S4D-E**). Similar restoration was also observed for Red1 (**Figure 3C**) (Sun et al., 2015), indicating that Scc1-cohesin is partly competent at restoring axis function in the absence of *REC8*.

Comparison of Smc4-PK9 enrichment at pericentromeres and axis sites along chromosome arms further revealed that the relative enrichment at arm sites depends partly on DSB formation. In wild-type, the condensin signal is somewhat higher in percentromeric regions compared to arm axis sites, but relative centromere enrichment was strongly increased in *spo11-YF* mutants (**Figure 3D**). Therefore, DSB formation promotes a proportionally higher association of condensin along chromosomes arms, in line with cytological observations (**Figure 1B** and **S1B**). Together, these results support the conclusions that cohesin-dependent chromosome architecture establishes binding sites for condensin during meiotic prophase, and that these sites become proportionally more occupied upon meiotic DSB formation.

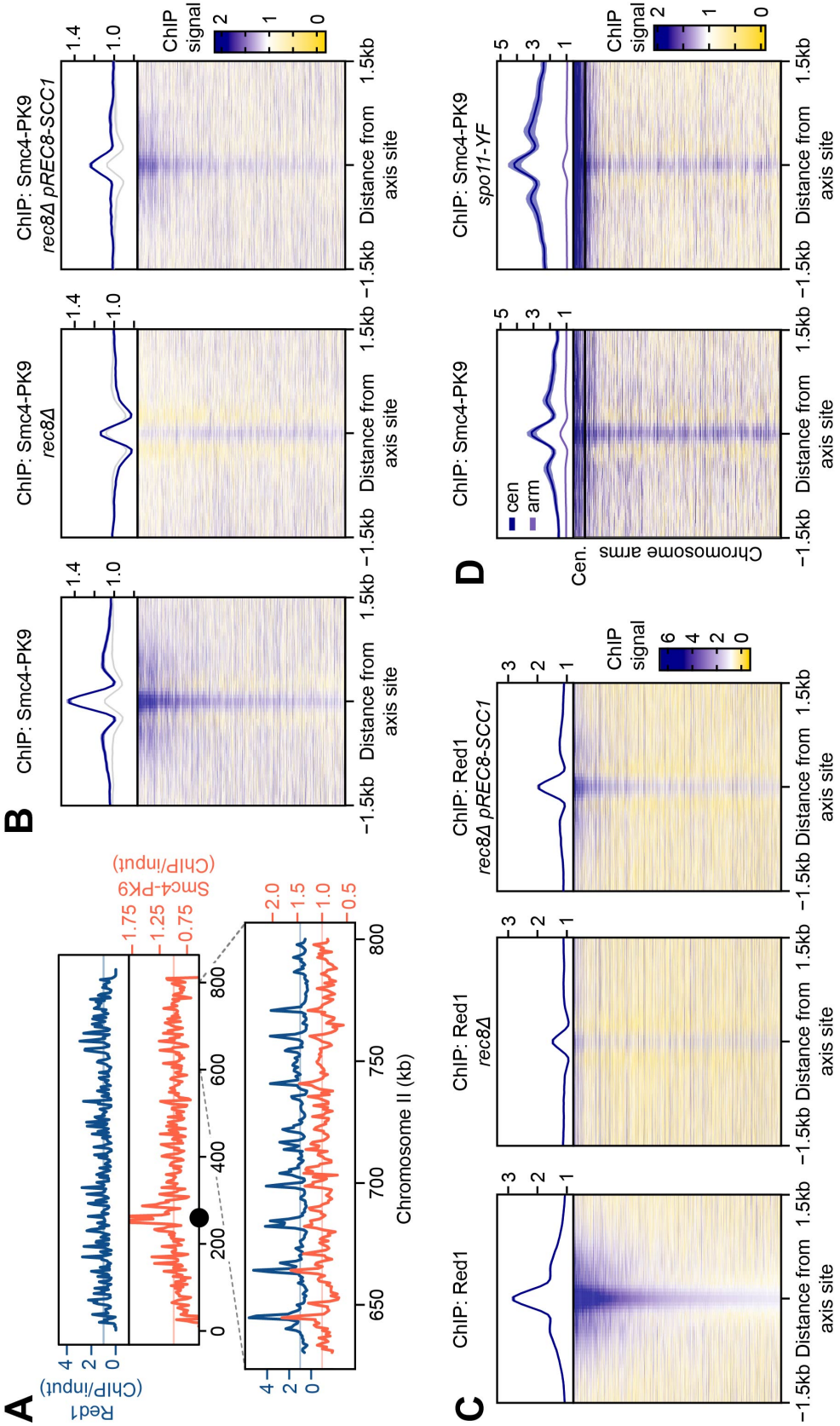

Figure 3. Condensin enrichment at axis sites requires cohesin. (A) Red1 (blue) [H119/6408] and Smc4-PK9 (pink) [H6408] binding pattern along chromosome II and a representative region (inset) in wild-type cells. Horizontal blue and pink lines represent genome average. **(B)** Heatmap of Smc4-PK9

enrichment around axis sites in wild type [H6408], *rec8*Δ [H7660]**,** and *rec8*Δ *pREC8-SCC1* mutants [H8921]. Axis sites are Red1 summits in wild-type cells with -log10 qvalue greater than or equal to 20, as determined by MACS2. ChIP-seq values were averaged over 50bp windows around axis sites across a 3kb window. Rows are sorted by amount of Red1 binding at these sites. Blue is high enrichment, gold is depletion. Mean and S.E.M. are shown in line graphs directly above heatmap. Gray line indicates mean and S.E.M. of the no-tag controls: H7797, H8428, and H8038, respectively. **(C)** Heatmap of Red1 enrichment around axis sites in a wild type, *rec8*Δ [H6200/H7660/H8151/H7772]**,** and *rec8*Δ *pREC8-SCC1* mutants [H8038]. **(D)** Smc4-PK9 enrichment at axis sites based upon proximity to centromeres in wild type and *spo11-YF* mutants [H8630]. The plots are created as in (B) but are sorted by distance to centromeres. The horizontal black line separates axis sites in the pericentromeric regions (30kb from centromeres) from more distal axis sites on chromosome arms. In the line graph above, dark blue is the mean and S.D. at axis sites within the pericentromic region, light purple shows mean and S.D. at the axis sites on the arms.

Condensin is enriched at DSB hotspots

Our ChIP-seq analyses revealed a subset of Smc4-PK9 peaks that did not overlap with axis attachment sites (**Figure 3A**). Further analysis showed that most of these peaks localized to divergent promoter regions (**Figure 4A**), which are common sites of meiotic DSB formation (Blitzblau et al., 2007, Pan et al., 2011). Similar enrichment is not observed in vegetative cells (**Figure S5**). We asked whether condensin at these sites is linked to DSB formation by analyzing Spo11-oligo data, which reports on the relative frequencies of DSB formation (Pan et al., 2011, Thacker et al., 2014). This analysis revealed a broad correlation between condensin enrichment and hotspot activity (**Figure 4B**).

The correlation with hotspot activity may either reflect differences in the chromosomal architecture of strong hotspots or a response to DSB formation *per se*. To distinguish between these possibilities, we analyzed Smc4-PK9 binding in mutants with altered DSB activity. *spo11-YF* mutants exhibited a relative reduction of Smc4-PK9 enrichment in divergent regions, including hotspots (**Figure 4C-D**), likely because little condensin leaves the nucleolus in these mutants (**Figure 1B**). By contrast, the correlation of condensin enrichment with wild-type hotspot activity was largely unchanged in the absence of *REC8* (**Figure 4E-F**), even though the meiotic DSB landscape is greatly altered in *rec8*Δ mutants (Sun et al., 2015, Kugou et al., 2009). These data imply that condensin enrichment at hotspots is unaffected by local DSB levels. Instead, condensin may respond to local chromatin features that also drive hotspot activity. These features appear to be independent of cohesin.

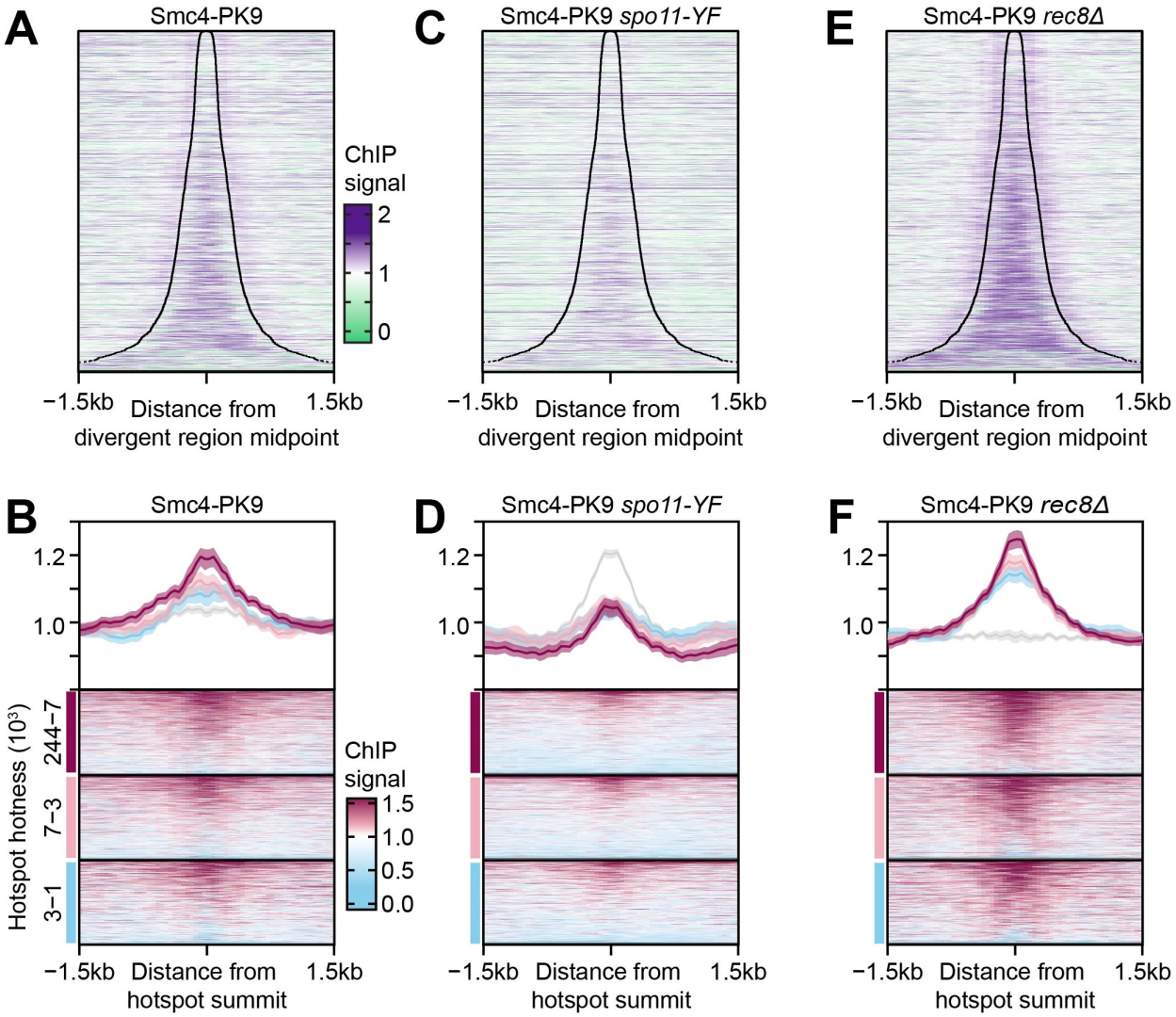

Figure 4. DSB-dependence of condensin binding pattern. (A) Smc4-PK9 enrichment around divergent gene pairs in meiotic prophase [H6408]. ChIP-seq values were averaged over 50bp windows around the midpoint of intergenic regions across a 3kb window. Rows were sorted by distance between genes. Black curved lines indicate translational start sites. Purple is high enrichment, turquoise is depletion. **(B)** Smc4-PK9 enrichment around DSB hotspots in wild-type cells. Hotspot locations and strengths are from (Thacker et al., 2014). Hotspots were placed into three quantiles grouped by strength (from hottest to weakest: maroon, pink, light blue). ChIP-seq values were averaged over 50bp windows around the midpoints of hotspots across a 3kb window. Rows in each quantile were sorted by Smc4-PK9 enrichment. Pink is high enrichment; light blue is depletion. Mean and S.E.M. are shown in line graph directly above heatmap. Gray line indicates mean and S.E.M. of the no-tag control [H7797]. Smc4-PK9 binding in *spo11-YF* mutants [H8630] at divergent gene pairs **(C)** and DSB hotspots **(D)**. Smc4-PK9 binding in *rec8*Δ mutants [H7660] at divergent gene pairs **(E)** and DSB hotspots **(F)**. No-tag controls were: H8643 (D) and H8428 (F).

Scc2 is required for condensin binding at pericentromeres and axis sites

Previous work had implicated the cohesin loader Scc2/NIPBL as a mediator of condensin loading in vegetative cells (D'Ambrosio et al., 2008), although this role remains controversial and is not observed in *C. elegans* (Shen and Skibbens, 2017, Lightfoot et al., 2011). To test whether Scc2 is required for condensin recruitment to meiotic prophase chromosomes, we utilized the "anchor away" system, in which proteins tagged with FRB become depleted from the nucleus in the presence of rapamycin (Haruki et al., 2008). In strains expressing Scc2-FRB, the addition of rapamycin at the time of meiotic induction led to a comprehensive loss of Smc4-PK9 ChIP-seq signal from pericentromeres and axis attachment sites (**Figure 5A-B**). Thus, Scc2 is required for condensin recruitment to these sites. The magnitude of this phenotype was surprising because depletion of Scc2-FRB only caused a partial depletion of cohesin from chromosomes (**Figure 5C** and **S6**), despite Scc2 being essential for cohesin loading (Ciosk et al., 2000). These data argue that the effect of Scc2 depletion on condensin recruitment is not secondary to a failure to load cohesin. They also imply that the pool of cohesin that remains upon Scc2 depletion does not efficiently mediate condensin recruitment to axis sites.

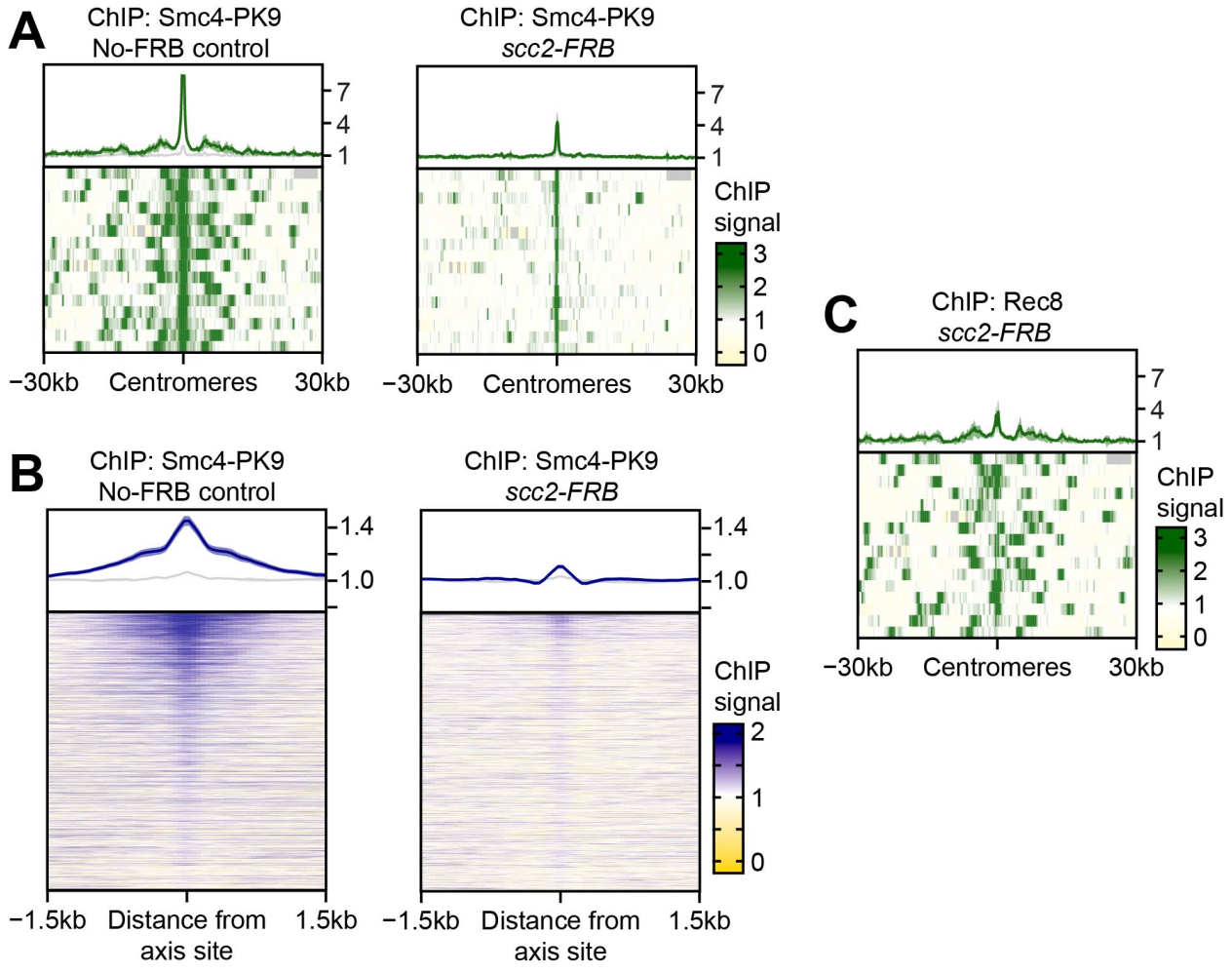

Figure 5. Scc2 is required for condensin binding at pericentromeres and axis sites. (A) Smc4-PK9 enrichment around centromeres in no-FRB control [H9724] and *scc2-FRB* [H9722] strains after rapamycin treatment. Plots were created as described in Figure 2. **(B)** Axis site binding of Smc4-PK9 in no-FRB control and *scc2-FRB* strains. Heatmaps and line plots were created like in Figure 3B. No-PK9-tag controls were H6978 and H9723 for the no-FRB control and *scc2-FRB* strains, respectively. **(C)** Rec8 enrichment around centromeres in the *scc2-FRB* after rapamycin treatment.

Condensin and Scc2 have similar binding patterns in meiosis

To determine whether Scc2 is in the appropriate chromosomal places to control condensin binding, we performed ChIP-seq analysis of Scc2 fused to 6HA. Scc2-6HA distribution along prophase chromosomes revealed many similarities with condensin. Scc2 was strongly enriched at core centromeres and pericentromeres (**Figure 6A**) as well as at axis attachment sites (**Figures 6B** and **S7A**). In addition, Scc2 was also enriched in divergent promoter regions during meiotic prophase (**Figure S7B**), consistent with similar observation in vegetative cells (Kogut et al., 2009).

Enrichment of Scc2 in the pericentromeric regions and at axis attachment sites was largely abolished in *rec8*Δ mutants, indicating that Scc2 binding at these sites depends on cohesin (**Figure 6C-D**). This observation contrasts with low-resolution ChIP-chip analyses, which found no dependence on cohesin (Lin et al., 2011). However, the dependence of Scc2 on cohesin was previously observed in the pericentromeres of vegetative cells (Fernius et al., 2013) and is consistent with recent analyses showing that Scc2 remains associated with the cohesin complex after loading to stimulate the ATPase activity of cohesin (Petela et al., 2018).

Finally, like condensin, the relative distribution of Scc2 along prophase chromosomes depends on meiotic DSB formation. Analysis of *spo11-YF* mutants revealed a strong enrichment of Scc2-HA around centromeres that was not observed in wild type (**Figure 6E**). Moreover, Scc2 binding to axis attachment sites was reduced compared to pericentromeres in the absence of DSB formation (**Figure 6F**). These changes in Scc2 distribution in response to DSB formation are remarkably similar to the DSB-dependent changes observed for condensin (**Figure 2F** and **3D**) and suggest that Scc2 redistribution upon DSB formation is responsible for the DSB-dependent recruitment of condensin to axis attachment sites.

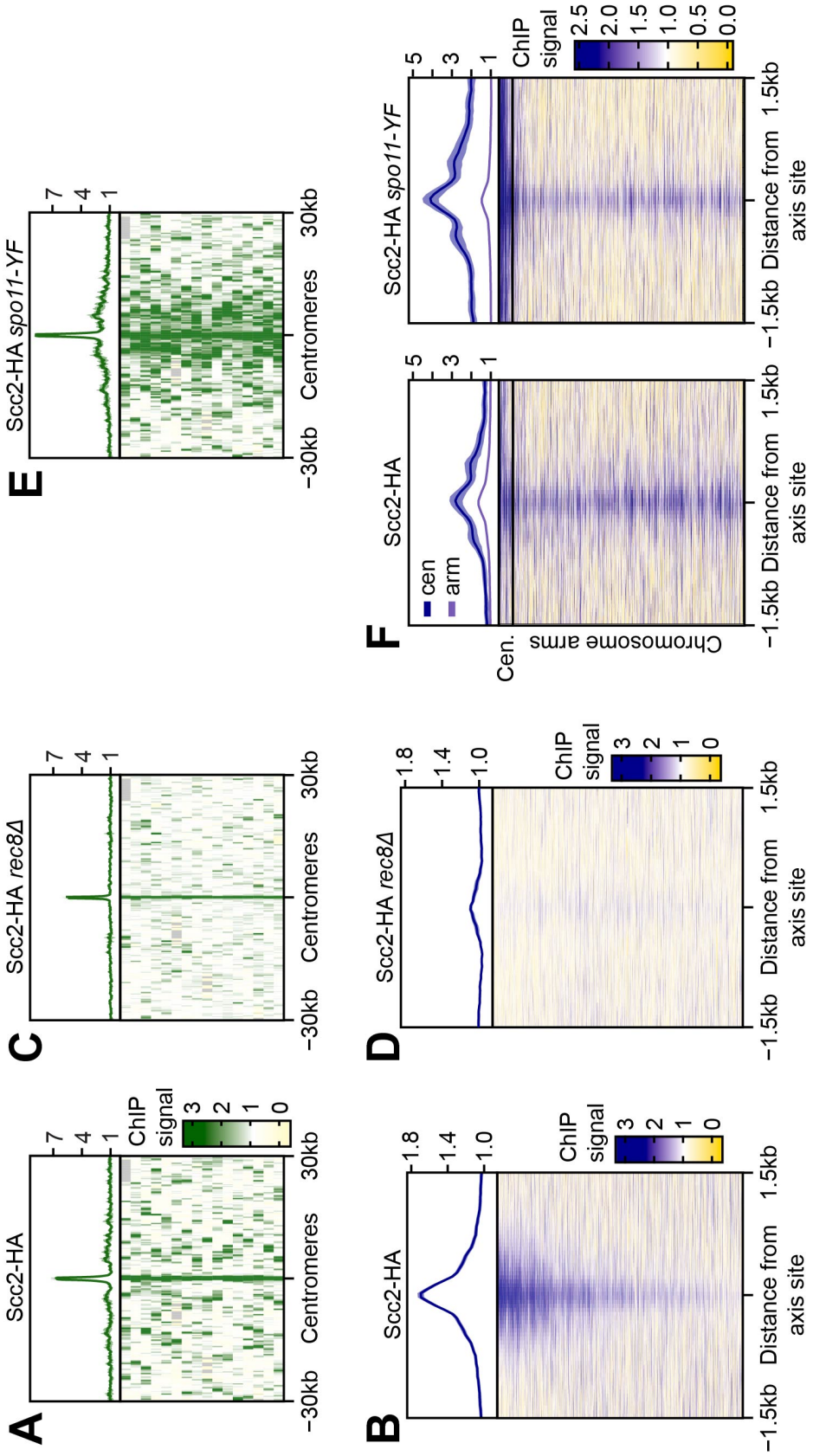

Figure 6. Scc2-HA binding patterns depend on *REC8* and *SPO11*. Scc2-HA binding at pericentromeres **(A)** and axis sites **(B)** in wild-type meiotic prophase cells (t=3h) [H8867]. Scc2-HA enrichment in *rec8*Δ mutants [H8869] at pericentromeres **(C)** and axis sites **(D)**. **(E)** Scc2-HA binding at

pericentromeres in *spo11-YF* mutants [H8868]. Detailed descriptions of the creation of panels A-E are in Figure 2 and Figure 3B. **(F)** Scc2-HA enrichment at axis sites based upon proximity to centromeres in wild type and *spo11-YF* mutants. Plots were created as described in Figure 3D.

Discussion

Condensin organizes chromosome architecture by dynamically interacting with chromosomes. Here, we analyzed the mechanisms governing condensin recruitment to meiotic chromosomes. We observed a broad redistribution of condensin in response to meiotic DSB formation depended on Scc2-cohesin.

Our analyses of meiotic prophase chromosomes revealed several enrichment patterns of condensin that, in vegetative cells, are only observed at the time of mitosis. These include strong condensin enrichment at pericentromeric cohesin-associated regions and binding in the TAD-like region between the rDNA and the centromere on chromosome XII (Lazar-Stefanita et al., 2017, Paul et al., 2018), and may reflect the high degree of longitudinal chromosome compaction during this stage of meiosis. It is unclear how meiotic prophase chromosomes achieve a mitotic-like state with respect to condensin binding, because the main mitotic driver kinases, M-CDK and Polo-like kinase, are not active in meiotic prophase (Carlile and Amon, 2008, Sourirajan and Lichten, 2008). Perhaps the program is driven by the activity of Ipl1/Aurora B kinase, which controls several processes in meiotic prophase (Newnham et al., 2013) and has been shown help target condensin to chromosome arms during mitosis (Tada et al., 2011).

We identified the cohesin loader and activator Scc2 as important for DSB-dependent recruitment of condensin to prophase chromosomes. The Scc2 dependence of condensin loading is in line with analyses of vegetative cells (D'Ambrosio et al., 2008), although the function of Scc2 as a condensin recruiter has recently been disputed based on analyses of rDNA compaction (Shen and Skibbens, 2017). However, condensin recruitment to the rDNA also requires rDNA-specific proteins (Johzuka and Horiuchi, 2009), which may represent an independent mode of condensin recruitment. Whether the function of Scc2 as a meiotic condensin recruiter is conserved in other organisms remains unclear. Scc2/NIPBL and condensin show similar kinetics of binding on mouse spermatocyte chromosomes (Visnes et al., 2014), but Scc2 has been excluded as a condensin recruiter on prophase chromosomes in *C. elegans* (Lightfoot et al., 2011). It should be noted that chromosome morphogenesis can occur in the absence of DSB formation in *C. elegans* (Dernburg et al., 1998), a situation that may enable additional mechanisms of condensin recruitment. Indeed, condensin binding to meiotic chromosomes in *C. elegans* and mice is

partially dependent on the SMC5/6 complex (Hong et al., 2016, Hwang et al., 2017), which may mask potential roles of Scc2/NIPBL in condensin loading.

Our data show that Scc2 redistributes in response to DSB formation in a pattern very similar to condensin and indicate that the DSB-dependent redistribution of condensin to the pericentromere and other axis sites is a consequence of Scc2 redistribution to those sites. An interesting aspect of this redistribution is the increased relative enrichment of both proteins at pericentromeres in the absence of DSBs. Similar pericentromeric enrichment has also been reported for Spo11 (Kugou et al., 2009) and the axis protein Hop1 (Subramanian et al., 2019), both of which become transiently enriched at pericentromeres in the earliest stages of meiotic prophase, before distributing to chromosome arms. Whether this initial enrichment at centromeres is functionally important for any of these proteins or simply reflects unique aspects of the pericentromeric regions, such as their early replication timing (Blitzblau et al., 2012), remains to be determined.

The combined redistribution of Scc2 and condensin upon DSB formation implies that prophase chromosome dynamics change fundamentally upon initiation of meiotic recombination. Scc2 can move between cohesin complexes and stimulate cohesin ATPase activity (Petela et al., 2018, Rhodes et al., 2017). Thus, the combined deployment of condensin and the ATPase-active form of cohesin is expected to strongly increase the dynamics of loop extrusion, which may be important for multiple aspects of meiotic recombination, including homology search and the correction of inappropriate repair interaction. A temporary increase in cohesin activity is also suggested in mouse by the elevated Scc2/NIPBL signal on chromosomes during meiotic recombination (Kuleszewicz et al., 2013, Visnes et al., 2014).

The two complexes likely have different functions during meiotic prophase. Cohesin is essential for forming the loop-axis architecture of meiotic chromosomes and the assembly of the axial element (Klein et al., 1999, Sun et al., 2015), whereas condensin may have a function in its stabilization (Yu and Koshland, 2003). Lack of cohesin causes severe defects in meiotic DSB repair (Klein et al., 1999, Kim et al., 2010), while lack of condensin has primarily been implicated in altered repair partner choice of persistent DSBs (Yu and Koshland, 2003). These different functions may be linked to different recruitment mechanisms but may also be connected to biochemical differences in loop extrusion dynamics (Golfier et al., 2020). Intriguingly, the two complexes also regulate each other ((Yu and Koshland, 2005, Hernandez et al., 2018) and this study). This interdependence may help balance SMC activities as needed to stimulate dynamic searches or stabilize interactions by taking advantage of

different relative loop extruding activities and residence times. Our data suggest that that the meiotic loop-axis architecture becomes increasingly dynamic upon meiotic DSB formation, which may be important for the faithful completion of meiotic recombination.

Methods

Yeast strains and growth conditions

All strains had an SK1 background unless indicated otherwise. A complete list is located in Table S1. Smc4-PK9 was transferred from W303 (D'Ambrosio et al., 2008) using allele replacement by transformation. Gene disruption and tagging were carried out using a PCR-based protocol (Longtine et al., 1998). Synchronous meiosis was induced as previously described (Sun et al., 2015). All samples were collected 3h after induction unless otherwise noted. For all time courses, efficient meiotic entry was confirmed by monitoring DNA content using flow cytometry. Only cultures that efficiently entered meiosis were analyzed. For anchor away experiments, rapamycin was added to a final concentration of 1nM at the time of meiotic induction (0h).

ChIP-seq

Chromatin immunoprecipitation was performed as described (Blitzblau et al., 2012). ChIP samples were derived from either 50mL of asynchronous culture at OD=1 or 25mL meiotic culture. Samples were immunoprecipitated with 2 µL anti-Red1 serum (Lot#16440, kind gift of N. Hollingsworth (Wan et al., 2004)), 2 µL anti-Rec8 serum (kind gift N. Hollingsworth (Prugar et al., 2017)), 20µL anti-V5 (PK9) agarose affinity gel (Sigma), or 10µL of anti-HA 3F10 (Roche Applied Science) antibody per IP. Library preparation was performed using Illumina TruSeq DNA Sample Prep Kits v1 but adapters were used at 1:20 dilution. Library quality was confirmed by Qubit HS assay kit and Agilent 2200 TapeStation. 51-bp sequencing was accomplished on an Illumina HiSeq 2500 or NextSeq 500 instrument.

PK9 specific adjustments to ChIP-seq protocol

PK9 antibody binding is enriched at nucleosome-free regions and other open DNA in the no-tag controls, many of which are known condensin binding sites (D'Ambrosio et al., 2008, Murillo-Pineda et al., 2014). To increase the concentration of reads from longer ChIPed fragments, ChIP and input DNA were re-sonicated using a Bioruptor Pico (Diagenode, NJ, USA) with the following settings: 30 secs ON and 30 secs OFF for 5 cycles. This change to the general ChIP-seq protocol is not novel (Mokry et al., 2010).

Data analysis

Sequencing reads were mapped to the SK1 genome (Yue et al., 2017) using Bowtie (Langmead et al., 2009). Reads that mapped to only one location without mismatches were used in further analyses. Further processing was completed using MACS-2.1.0 (https://github.com/taoliu/MACS) (Zhang et al., 2008). Single end reads were extended towards 3' ends to a final length of 200bp, and probabilistically determined PCR duplications were removed. Pileups of both the input and ChIP libraries were SPMR-normalized (signal per million reads), followed by a calculation of the fold-enrichment of the ChIP data over the input data. Before plotting, all data was normalized to produce a genome average of 1 to allow for some comparability between experiments. When available, reads of biological replicates were combined prior to MACS2 analysis. For analysis of the rDNA, reads were mapped to a single rDNA repeat using Bowtie with default settings.

Chromosome spreads

Meiotic nuclear spreads were performed as described (Subramanian et al., 2016). GFP was detected using polyclonal chicken anti-GFP (abcam) at 1:200 and Alexa Fluor 488 anti-chicken at 1:100. Zip1 was detected using Zip1 yC-19 goat antibody (Santa Cruz Biotechnology) at 1:200 and anti-goat Cy3 at 1:200. Nop1 was detected using mouse monoclonal Nop1 antibody (EnCor Biotechnology) at 1:400 and anti-mouse Cy3 at 1:200. All secondary antibodies came from Jackson ImmunoResearch. Images were obtained as described (Subramanian et al., 2016) and analyzed using softWoRx 5.0 software.

Acknowledgements

We thank F. Uhlmann and N. Hollingsworth for sharing strains and antibodies, H. Murakami for helpful discussions, and the NYU Department of Biology Sequencing Core for technical assistance and data processing. This work was supported by the National Institutes of Health [GM123035 to AH].

Author contributions

Conceptualization, T.E.M and A.H.; Investigation, T.E.M., J.H. and A.H.; Software, T.E.M.; Formal Analysis, T.E.M., J.H. and A.H.; Writing – Original Draft, T.E.M and A.H.; Writing – Review & Editing, T.E.M, J.H., and A.H.

Conflict of Interest

The authors declare no conflict of interest.

Data Availability

The datasets and computer code produced in this study are available in following databases:

- Meiotic ChIP-seq data: Gene Expression Omnibus GSEXXXXXX 'https://www.ncbi.nlm.nih.gov/geo/query/acc.cgi?acc=GSEXXXXXX'
- Computer scripts for processing Illumina reads: Github 'https://github.com/hochwagenlab/ChIPseq_functions/tree/master/ChIPseq_Pipeline_v3/'

The analysis of condensin in asynchronous cells used previously published ChIP-seq data: GEO accession GSE106104 'https://www.ncbi.nlm.nih.gov/geo/query/acc.cgi?acc=GSE106104'

References

AUERBACH, R. K., EUSKIRCHEN, G., ROZOWSKY, J., LAMARRE-VINCENT, N., MOQTADERI, Z., LEFRANCOIS, P., STRUHL, K., GERSTEIN, M. & SNYDER, M. 2009. Mapping accessible chromatin regions using Sono-Seq. *Proc Natl Acad Sci U S A,* 106**,** 14926-31.

BERGERAT, A., DE MASSY, B., GADELLE, D., VAROUTAS, P. C., NICOLAS, A. & FORTERRE, P. 1997. An atypical topoisomerase II from Archaea with implications for meiotic recombination. *Nature,* 386**,** 414-7.

BICKMORE, W. A. & VAN STEENSEL, B. 2013. Genome architecture: domain organization of interphase chromosomes. *Cell,* 152**,** 1270-84.

BLITZBLAU, H. G., BELL, G. W., RODRIGUEZ, J., BELL, S. P. & HOCHWAGEN, A. 2007. Mapping of meiotic single-stranded DNA reveals double-stranded-break hotspots near centromeres and telomeres. *Curr Biol,* 17**,** 2003-12.

BLITZBLAU, H. G., CHAN, C. S., HOCHWAGEN, A. & BELL, S. P. 2012. Separation of DNA replication from the assembly of break-competent meiotic chromosomes. *PLoS Genet,* 8**,** e1002643.

BRAR, G. A., HOCHWAGEN, A., EE, L. S. & AMON, A. 2009. The multiple roles of cohesin in meiotic chromosome morphogenesis and pairing. *Mol Biol Cell,* 20**,** 1030-47.

BURRACK, L. S., APPLEN CLANCEY, S. E., CHACON, J. M., GARDNER, M. K. & BERMAN, J. 2013. Monopolin recruits condensin to organize centromere DNA and repetitive DNA sequences. *Mol Biol Cell,* 24**,** 2807-19.

CABURET, S., ARBOLEDA, V. A., LLANO, E., OVERBEEK, P. A., BARBERO, J. L., OKA, K., HARRISON, W., VAIMAN, D., BEN-NERIAH, Z., GARCIA-TUNON, I., FELLOUS, M., PENDAS, A. M., VEITIA, R. A. & VILAIN, E. 2014. Mutant cohesin in premature ovarian failure. *N Engl J Med,* 370**,** 943-949.

CARLILE, T. M. & AMON, A. 2008. Meiosis I is established through division-specific translational control of a cyclin. *Cell,* 133**,** 280-91.

CIOSK, R., SHIRAYAMA, M., SHEVCHENKO, A., TANAKA, T., TOTH, A., SHEVCHENKO, A. & NASMYTH, K. 2000. Cohesin's binding to chromosomes depends on a separate complex consisting of Scc2 and Scc4 proteins. *Mol Cell,* 5**,** 243-54.

D'AMBROSIO, C., SCHMIDT, C. K., KATOU, Y., KELLY, G., ITOH, T., SHIRAHIGE, K. & UHLMANN, F. 2008. Identification of cis-acting sites for condensin loading onto budding yeast chromosomes. *Genes Dev,* 22**,** 2215-27.

DERNBURG, A. F., MCDONALD, K., MOULDER, G., BARSTEAD, R., DRESSER, M. & VILLENEUVE, A. M. 1998. Meiotic recombination in C. elegans initiates by a conserved mechanism and is dispensable for homologous chromosome synapsis. *Cell,* 94**,** 387-98.

FALK, J. E., CHAN, A. C., HOFFMANN, E. & HOCHWAGEN, A. 2010. A Mec1- and PP4-dependent checkpoint couples centromere pairing to meiotic recombination. *Dev Cell,* 19**,** 599-611.

FERNIUS, J., NERUSHEVA, O. O., GALANDER, S., ALVES FDE, L., RAPPSILBER, J. & MARSTON, A. L. 2013. Cohesin-dependent association of scc2/4 with the centromere initiates pericentromeric cohesion establishment. *Curr Biol,* 23**,** 599-606.

GEISINGER, A. & BENAVENTE, R. 2016. Mutations in Genes Coding for Synaptonemal Complex Proteins and Their Impact on Human Fertility. *Cytogenet Genome Res,* 150**,** 77-85.

GLYNN, E. F., MEGEE, P. C., YU, H. G., MISTROT, C., UNAL, E., KOSHLAND, D. E., DERISI, J. L. & GERTON, J. L. 2004. Genome-wide mapping of the cohesin complex in the yeast Saccharomyces cerevisiae. *PLoS Biol,* 2**,** E259.

GOLFIER, S., QUAIL, T., KIMURA, H. & BRUGUES, J. 2020. Cohesin and condensin extrude DNA loops in a cell-cycle dependent manner. *Elife,* 9.

HARUKI, H., NISHIKAWA, J. & LAEMMLI, U. K. 2008. The anchor-away technique: rapid, conditional establishment of yeast mutant phenotypes. *Mol Cell,* 31**,** 925-32.
HASSLER, M., SHALTIEL, I. A. & HAERING, C. H. 2018. Towards a Unified Model of SMC Complex Function. *Curr Biol,* 28**,** R1266-R1281.
HERNANDEZ, M. R., DAVIS, M. B., JIANG, J., BROUHARD, E. A., SEVERSON, A. F. & CSANKOVSZKI, G. 2018. Condensin I protects meiotic cohesin from WAPL-1 mediated removal. *PLoS Genet,* 14**,** e1007382.
HILDEBRAND, E. M. & DEKKER, J. 2020. Mechanisms and Functions of Chromosome Compartmentalization. *Trends Biochem Sci,* 45**,** 385-396.
HONG, Y., SONNEVILLE, R., AGOSTINHO, A., MEIER, B., WANG, B., BLOW, J. J. & GARTNER, A. 2016. The SMC-5/6 Complex and the HIM-6 (BLM) Helicase Synergistically Promote Meiotic Recombination Intermediate Processing and Chromosome Maturation during Caenorhabditis elegans Meiosis. *PLoS Genet,* 12**,** e1005872.
HWANG, G., SUN, F., O'BRIEN, M., EPPIG, J. J., HANDEL, M. A. & JORDAN, P. W. 2017. SMC5/6 is required for the formation of segregation-competent bivalent chromosomes during meiosis I in mouse oocytes. *Development,* 144**,** 1648-1660.
JIN, H., GUACCI, V. & YU, H. G. 2009. Pds5 is required for homologue pairing and inhibits synapsis of sister chromatids during yeast meiosis. *J Cell Biol,* 186**,** 713-25.
JOHANSEN, P. & CAM, H. P. 2015. Suppression of Meiotic Recombination by CENP-B Homologs in Schizosaccharomyces pombe. *Genetics,* 201**,** 897-904.
JOHZUKA, K. & HORIUCHI, T. 2009. The cis element and factors required for condensin recruitment to chromosomes. *Mol Cell,* 34**,** 26-35.
KEENEY, S., GIROUX, C. N. & KLECKNER, N. 1997. Meiosis-specific DNA double-strand breaks are catalyzed by Spo11, a member of a widely conserved protein family. *Cell,* 88**,** 375-84.
KIM, K. P., WEINER, B. M., ZHANG, L., JORDAN, A., DEKKER, J. & KLECKNER, N. 2010. Sister cohesion and structural axis components mediate homolog bias of meiotic recombination. *Cell,* 143**,** 924-37.
KLEIN, F., MAHR, P., GALOVA, M., BUONOMO, S. B., MICHAELIS, C., NAIRZ, K. & NASMYTH, K. 1999. A central role for cohesins in sister chromatid cohesion, formation of axial elements, and recombination during yeast meiosis. *Cell,* 98**,** 91-103.
KOGUT, I., WANG, J., GUACCI, V., MISTRY, R. K. & MEGEE, P. C. 2009. The Scc2/Scc4 cohesin loader determines the distribution of cohesin on budding yeast chromosomes. *Genes Dev,* 23**,** 2345-57.
KUGOU, K., FUKUDA, T., YAMADA, S., ITO, M., SASANUMA, H., MORI, S., KATOU, Y., ITOH, T., MATSUMOTO, K., SHIBATA, T., SHIRAHIGE, K. & OHTA, K. 2009. Rec8 guides canonical Spo11 distribution along yeast meiotic chromosomes. *Mol Biol Cell,* 20**,** 3064-76.
KULESZEWICZ, K., FU, X. & KUDO, N. R. 2013. Cohesin loading factor Nipbl localizes to chromosome axes during mammalian meiotic prophase. *Cell Div,* 8**,** 12.
LACZIK, M., HENDRICKX, J., VEILLARD, A. C., TAMMOH, M., MARZI, S. & PONCELET, D. 2016. Iterative Fragmentation Improves the Detection of ChIP-seq Peaks for Inactive Histone Marks. *Bioinform Biol Insights,* 10**,** 209-224.
LANGMEAD, B., TRAPNELL, C., POP, M. & SALZBERG, S. L. 2009. Ultrafast and memory-efficient alignment of short DNA sequences to the human genome. *Genome Biol,* 10**,** R25.
LAZAR-STEFANITA, L., SCOLARI, V. F., MERCY, G., MULLER, H., GUERIN, T. M., THIERRY, A., MOZZICONACCI, J. & KOSZUL, R. 2017. Cohesins and condensins orchestrate the 4D dynamics of yeast chromosomes during the cell cycle. *EMBO J,* 36**,** 2684-2697.
LENGRONNE, A., KATOU, Y., MORI, S., YOKOBAYASHI, S., KELLY, G. P., ITOH, T., WATANABE, Y., SHIRAHIGE, K. & UHLMANN, F. 2004. Cohesin relocation from sites of chromosomal loading to places of convergent transcription. *Nature,* 430**,** 573-8.

LI, P., JIN, H. & YU, H. G. 2014. Condensin suppresses recombination and regulates double-strand break processing at the repetitive ribosomal DNA array to ensure proper chromosome segregation during meiosis in budding yeast. *Mol Biol Cell,* 25**,** 2934-47.

LIGHTFOOT, J., TESTORI, S., BARROSO, C. & MARTINEZ-PEREZ, E. 2011. Loading of meiotic cohesin by SCC-2 is required for early processing of DSBs and for the DNA damage checkpoint. *Curr Biol,* 21**,** 1421-30.

LIN, W., JIN, H., LIU, X., HAMPTON, K. & YU, H. G. 2011. Scc2 regulates gene expression by recruiting cohesin to the chromosome as a transcriptional activator during yeast meiosis. *Mol Biol Cell,* 22**,** 1985-96.

LLANO, E., GOMEZ, H. L., GARCIA-TUNON, I., SANCHEZ-MARTIN, M., CABURET, S., BARBERO, J. L., SCHIMENTI, J. C., VEITIA, R. A. & PENDAS, A. M. 2014. STAG3 is a strong candidate gene for male infertility. *Hum Mol Genet,* 23**,** 3421-31.

LONGTINE, M. S., MCKENZIE, A., 3RD, DEMARINI, D. J., SHAH, N. G., WACH, A., BRACHAT, A., PHILIPPSEN, P. & PRINGLE, J. R. 1998. Additional modules for versatile and economical PCR-based gene deletion and modification in Saccharomyces cerevisiae. *Yeast,* 14**,** 953-61.

MARKOWITZ, T. E., SUAREZ, D., BLITZBLAU, H. G., PATEL, N. J., MARKHARD, A. L., MACQUEEN, A. J. & HOCHWAGEN, A. 2017. Reduced dosage of the chromosome axis factor Red1 selectively disrupts the meiotic recombination checkpoint in Saccharomyces cerevisiae. *PLoS Genet,* 13**,** e1006928.

MCNICOLL, F., STEVENSE, M. & JESSBERGER, R. 2013. Cohesin in gametogenesis. *Curr Top Dev Biol,* 102**,** 1-34.

METS, D. G. & MEYER, B. J. 2009. Condensins regulate meiotic DNA break distribution, thus crossover frequency, by controlling chromosome structure. *Cell,* 139**,** 73-86.

MOKRY, M., HATZIS, P., DE BRUIJN, E., KOSTER, J., VERSTEEG, R., SCHUIJERS, J., VAN DE WETERING, M., GURYEV, V., CLEVERS, H. & CUPPEN, E. 2010. Efficient double fragmentation ChIP-seq provides nucleotide resolution protein-DNA binding profiles. *PLoS One,* 5**,** e15092.

MURILLO-PINEDA, M., CABELLO-LOBATO, M. J., CLEMENTE-RUIZ, M., MONJE-CASAS, F. & PRADO, F. 2014. Defective histone supply causes condensin-dependent chromatin alterations, SAC activation and chromosome decatenation impairment. *Nucleic Acids Res,* 42**,** 12469-82.

NEWNHAM, L., JORDAN, P. W., CARBALLO, J. A., NEWCOMBE, S. & HOFFMANN, E. 2013. Ipl1/Aurora kinase suppresses S-CDK-driven spindle formation during prophase I to ensure chromosome integrity during meiosis. *PLoS One,* 8**,** e83982.

OCAMPO-HAFALLA, M., MUNOZ, S., SAMORA, C. P. & UHLMANN, F. 2016. Evidence for cohesin sliding along budding yeast chromosomes. *Open Biol,* 6.

PAN, J., SASAKI, M., KNIEWEL, R., MURAKAMI, H., BLITZBLAU, H. G., TISCHFIELD, S. E., ZHU, X., NEALE, M. J., JASIN, M., SOCCI, N. D., HOCHWAGEN, A. & KEENEY, S. 2011. A hierarchical combination of factors shapes the genome-wide topography of yeast meiotic recombination initiation. *Cell,* 144**,** 719-31.

PAUL, M. R., MARKOWITZ, T. E., HOCHWAGEN, A. & ERCAN, S. 2018. Condensin Depletion Causes Genome Decompaction Without Altering the Level of Global Gene Expression in Saccharomyces cerevisiae. *Genetics,* 210**,** 331-344.

PETELA, N. J., GLIGORIS, T. G., METSON, J., LEE, B. G., VOULGARIS, M., HU, B., KIKUCHI, S., CHAPARD, C., CHEN, W., RAJENDRA, E., SRINIVISAN, M., YU, H., LOWE, J. & NASMYTH, K. A. 2018. Scc2 Is a Potent Activator of Cohesin's ATPase that Promotes Loading by Binding Scc1 without Pds5. *Mol Cell,* 70**,** 1134-1148 e7.

PRUGAR, E., BURNETT, C., CHEN, X. & HOLLINGSWORTH, N. M. 2017. Coordination of Double Strand Break Repair and Meiotic Progression in Yeast by a Mek1-Ndt80 Negative Feedback Loop. *Genetics,* 206**,** 497-512.

RHODES, J., MAZZA, D., NASMYTH, K. & UPHOFF, S. 2017. Scc2/Nipbl hops between chromosomal cohesin rings after loading. *Elife,* 6.
SCHALBETTER, S. A., FUDENBERG, G., BAXTER, J., POLLARD, K. S. & NEALE, M. J. 2019. Principles of meiotic chromosome assembly revealed in S. cerevisiae. *Nat Commun,* 10**,** 4795.
SCHALBETTER, S. A., GOLOBORODKO, A., FUDENBERG, G., BELTON, J. M., MILES, C., YU, M., DEKKER, J., MIRNY, L. & BAXTER, J. 2017. SMC complexes differentially compact mitotic chromosomes according to genomic context. *Nat Cell Biol,* 19**,** 1071-1080.
SHEN, D. & SKIBBENS, R. V. 2017. Chl1 DNA helicase and Scc2 function in chromosome condensation through cohesin deposition. *PLoS One,* 12**,** e0188739.
SOURIRAJAN, A. & LICHTEN, M. 2008. Polo-like kinase Cdc5 drives exit from pachytene during budding yeast meiosis. *Genes Dev,* 22**,** 2627-32.
SUBRAMANIAN, V. V., MACQUEEN, A. J., VADER, G., SHINOHARA, M., SANCHEZ, A., BORDE, V., SHINOHARA, A. & HOCHWAGEN, A. 2016. Chromosome Synapsis Alleviates Mek1-Dependent Suppression of Meiotic DNA Repair. *PLoS Biol,* 14**,** e1002369.
SUBRAMANIAN, V. V., ZHU, X., MARKOWITZ, T. E., VALE-SILVA, L. A., SAN-SEGUNDO, P. A., HOLLINGSWORTH, N. M., KEENEY, S. & HOCHWAGEN, A. 2019. Persistent DNA-break potential near telomeres increases initiation of meiotic recombination on short chromosomes. *Nat Commun,* 10**,** 970.
SUN, X., HUANG, L., MARKOWITZ, T. E., BLITZBLAU, H. G., CHEN, D., KLEIN, F. & HOCHWAGEN, A. 2015. Transcription dynamically patterns the meiotic chromosome-axis interface. *Elife,* 4.
TADA, K., SUSUMU, H., SAKUNO, T. & WATANABE, Y. 2011. Condensin association with histone H2A shapes mitotic chromosomes. *Nature,* 474**,** 477-83.
THACKER, D., MOHIBULLAH, N., ZHU, X. & KEENEY, S. 2014. Homologue engagement controls meiotic DNA break number and distribution. *Nature,* 510**,** 241-6.
THADANI, R., KAMENZ, J., HEEGER, S., MUNOZ, S. & UHLMANN, F. 2018. Cell-Cycle Regulation of Dynamic Chromosome Association of the Condensin Complex. *Cell Rep,* 23**,** 2308-2317.
TRELLES-STICKEN, E., ADELFALK, C., LOIDL, J. & SCHERTHAN, H. 2005. Meiotic telomere clustering requires actin for its formation and cohesin for its resolution. *J Cell Biol,* 170**,** 213-23.
UHLMANN, F. 2016. SMC complexes: from DNA to chromosomes. *Nat Rev Mol Cell Biol,* 17**,** 399-412.
VAN RUITEN, M. S. & ROWLAND, B. D. 2018. SMC Complexes: Universal DNA Looping Machines with Distinct Regulators. *Trends Genet,* 34**,** 477-487.
VERZIJLBERGEN, K. F., NERUSHEVA, O. O., KELLY, D., KERR, A., CLIFT, D., DE LIMA ALVES, F., RAPPSILBER, J. & MARSTON, A. L. 2014. Shugoshin biases chromosomes for biorientation through condensin recruitment to the pericentromere. *Elife,* 3**,** e01374.
VIERA, A., GOMEZ, R., PARRA, M. T., SCHMIESING, J. A., YOKOMORI, K., RUFAS, J. S. & SUJA, J. A. 2007. Condensin I reveals new insights on mouse meiotic chromosome structure and dynamics. *PLoS One,* 2**,** e783.
VISNES, T., GIORDANO, F., KUZNETSOVA, A., SUJA, J. A., LANDER, A. D., CALOF, A. L. & STROM, L. 2014. Localisation of the SMC loading complex Nipbl/Mau2 during mammalian meiotic prophase I. *Chromosoma,* 123**,** 239-52.
WAN, L., DE LOS SANTOS, T., ZHANG, C., SHOKAT, K. & HOLLINGSWORTH, N. M. 2004. Mek1 kinase activity functions downstream of RED1 in the regulation of meiotic double strand break repair in budding yeast. *Mol Biol Cell,* 15**,** 11-23.
WANG, B. D., EYRE, D., BASRAI, M., LICHTEN, M. & STRUNNIKOV, A. 2005. Condensin binding at distinct and specific chromosomal sites in the Saccharomyces cerevisiae genome. *Mol Cell Biol,* 25**,** 7216-25.

YATSKEVICH, S., RHODES, J. & NASMYTH, K. 2019. Organization of Chromosomal DNA by SMC Complexes. *Annu Rev Genet,* 53**,** 445-482.

YU, H. G. & KOSHLAND, D. 2005. Chromosome morphogenesis: condensin-dependent cohesin removal during meiosis. *Cell,* 123**,** 397-407.

YU, H. G. & KOSHLAND, D. E. 2003. Meiotic condensin is required for proper chromosome compaction, SC assembly, and resolution of recombination-dependent chromosome linkages. *J Cell Biol,* 163**,** 937-47.

YUE, J. X., LI, J., AIGRAIN, L., HALLIN, J., PERSSON, K., OLIVER, K., BERGSTROM, A., COUPLAND, P., WARRINGER, J., LAGOMARSINO, M. C., FISCHER, G., DURBIN, R. & LITI, G. 2017. Contrasting evolutionary genome dynamics between domesticated and wild yeasts. *Nat Genet,* 49**,** 913-924.

ZHANG, Y., LIU, T., MEYER, C. A., EECKHOUTE, J., JOHNSON, D. S., BERNSTEIN, B. E., NUSBAUM, C., MYERS, R. M., BROWN, M., LI, W. & LIU, X. S. 2008. Model-based analysis of ChIP-Seq (MACS). *Genome Biol,* 9**,** R137.

ZICKLER, D. & KLECKNER, N. 2015. Recombination, Pairing, and Synapsis of Homologs during Meiosis. *Cold Spring Harb Perspect Biol,* 7.